

Supporting Information

Mechanistic Design of Chemically Diverse Polymers with Applications in Oral Drug Delivery

Laura I. Mosquera-Giraldo¹, Carlos H. Borca², Xiangtao Meng³, Kevin J. Edgar³, Lyudmila V. Slipchenko², and Lynne S. Taylor^{1,}*

¹Department of Industrial and Physical Pharmacy, College of Pharmacy, Purdue University, West Lafayette, Indiana, USA

²Department of Chemistry, College of Science, Purdue University, West Lafayette, Indiana, USA

³Department of Sustainable Biomaterials, College of Natural Resources and Environment, Virginia Tech, Blacksburg, Virginia, USA

Content

1. Description of the physicochemical properties for the newly synthesized cellulose polymers.
2. Description of experimental design of nucleation induction time experiments
3. Methodology for polymer characterization
4. Monomers conformations

1) Description of the physicochemical properties for the newly synthesized polymers

Table S1. Degree of substitution (DS), solubility parameter (SP), molecular weight (MW), and dispersity (Đ) for newly synthesized cellulose polymers.

#	Polymer abbreviation	DS (R ₁)	DS (R ₂)	DS (R ₃)	DS (OH)	R ₁	R ₂	R ₃	SP (MPa ^{1/2}) _a	Tg (°C)	Mw (kDa)	Đ	Solvent
1	CP-Tod-202	2.02	0.98	-	-	TOD	Pr	-	20.67	21	82.6	-	THF
2	CAB-Adp-081	0.81	1.99	0.14	0.06	Adp	Bu	Ac	22.08	82	9.5	-	THF
3	CAP-Adp-085	0.85	2.09	0.04	0.02	Adp	Pr	Ac	22.46	110	9.7	-	THF
4	CAP-Seb-024	0.24	2.09	0.04	0.63	Seb	Pr	Ac	23.04	116	18.8	-	THF
5	CA-Sub-090	0.9	1.82	-	0.28	Sub	Ac	-	23.18	81	21.2	-	THF
6	CA-Adp-067	0.67	1.82	-	0.51	Adp	Ac	-	24.21	134	20.5	-	THF
7	CA-Adp-056	0.56	1.82	-	0.62	Adp	Ac	-	24.47	154	60.3	1.60	THF ^b
8	CA-A1a-056	0.56	1.82	-	0.62	A1a	Ac	-	25.21	138	37.8	1.89	THF ^b
9	CAP-A1b-057	0.57	2.09	0.04	0.30	A1b	Pr	Ac	22.46	70	13.6	2.75	THF ^b
10	CAB-A1b-059	0.59	1.99	0.14	0.28	A1b	Bu	Ac	22.03	53	50.7	3.37	THF ^b
11	CA-A2a-079	0.79	1.82	-	0.39	A2a	Ac	-	25.42	124	37	1.43	DMSO
12	CA-A2b-067	0.67	1.82	-	0.51	A2b	Ac	-	22.95	139	38.2	1.67	THF ^b
13	CA-A3-056	0.56	1.82	-	0.62	A3	Ac	-	21.66	76	180	1.55	THF ^b
14	CA-A4-056	0.56	1.82	-	0.62	A4	Ac	-	25.02	41	100	1.78	THF ^b
15	CA-A5a-079	0.79	1.82	-	0.39	A5a	Ac	-	25.54	63	-	-	DMSO
16	CA-A5b-067	0.67 ^c	1.82	-	0.51	A5b	Ac	-	24.29	6 ^d , 89	-	-	DMSO
17	CA-A6-067	0.67	1.82	-	0.51	A6	Ac	-	21.40	88	-	-	DMSO
18	CA-A7-067	0.67	1.82	-	0.51	A7	Ac	-	21.83	103	-	-	DMSO

^aSolubility parameter (SP) calculation does not account for ionization ^bMaximum concentration of polymer achievable was 5 µg/mL. Even though the polymer is soluble in organic solvent at higher concentrations, it was observed to precipitate upon contact with water. Therefore, those

polymers were only tested at 5 $\mu\text{g/mL}$. ^cDue to the partial conversion (87%) of the reaction,¹ the actual DS of A5b is 0.58, with DS of A4b 0.09. ^dThe lower temperature endothermal transition was attributed to the segmental movement of the sidechain. **Nomenclature rules:** The polymer abbreviations in this manuscript follow a format XX-Xxx-000 (e.g. CA-A1a-056). In the first part XX represents the starting cellulose ester used. For example, CA denotes cellulose acetate ($\text{DS}_{\text{Ac}} = 1.82$) and CP denotes cellulose propionate ($\text{DS}_{\text{pr}} = 0.98$), as indicated in the table. The middle part Xxx denotes the functional side chain and digits in the last part denotes the DS of the side chain. For example, in CA-A1a-056; A1a denotes the functional group is A1a as shown in Figure 1, and the number 056 denotes the DS of A1a is 0.56.

Table S2. Polymer abbreviations for newly synthesized materials.

#	Polymer abbreviation	Equivalent abbreviation
1	CP-Tod-202	CP-Tod-202
2	CAB-Adp-081	CAB Adp 0.81
3	CAP-Adp-085	CAP Adp 0.85
4	CAP-Seb-024	CAP Seb 0.24
5	CA-Sub-090	CA 320S Sub 0.9
6	CA-Adp-067	CA 320S Adp 0.67
7	CA-Adp-056	CA-Pen056-AA-H
8	CA-A1a-056	CA-Pen056-Hb
9	CAP-A1b-057	CAP-Un057-Hb
10	CAB-A1b-059	CAB-Un059-Hb
11	CA-A2a-079	CA-Pen079-Aam-H
12	CA-A2b-067	CA-Un067-Aam-H
13	CA-A3-056	CA-Pen056-PEG-H
14	CA-A4-056	CA-Pen056-HEA-H
15	CA-A5a-079	CA-Pen079-HEA-3MPA
16	CA-A5b-067	CA-Un067-HEA-3MPA
17	CA-A7-067	CA-Un067-TMA-2ME
18	CA-A6-067	CA-Un067-TMA-3MPA

2) Description of experimental design of nucleation induction time experiments.

Telaprevir is used in the treatment of hepatitis C and it is formulated as an amorphous solid dispersion (ASD) due to its poor aqueous solubility.² It has been previously reported that when

the telaprevir concentration in solution exceeds ~90 -100 µg/ml a drug-rich phase is created, which consists of spherical aggregates with sizes in the range of 200 - 400 nm. This second phase is glassy in nature due to the high temperature glass transition of telaprevir. Consequently, the process of phase separation which occurs when the binodal concentration is exceeded is termed glass-liquid phase separation (GLPS).^{3, 4} The presence of a second phase is likely to impact nucleation kinetics, through providing interfaces for heterogeneous nucleation, and therefore it is important to evaluate the nucleation inhibition of polymers at supersaturations below and above GLPS. The nucleation inhibition is evaluated in a homogeneous solution (molecularly dissolved drug) and a two phase solution (molecularly dissolved drug and drug-rich particles). It has been demonstrated that ASDs can dissolve to yield solutions containing both molecularly dissolved drug and drug-rich aggregates, so this is an important consideration. A schematic of the experimental design is shown in Figure S1. The presence of amorphous aggregates in solution was visualized by cryo-scanning electron microscopy (cryo-SEM).

Induction times were determined using UV absorption and extinction measurements. In Figure S2, examples of typical absorption and light scattering profiles for supersaturated telaprevir solutions are shown. At concentration below GLPS, where the solution is initially homogeneous and contains molecularly dissolved drug, a simultaneous increase in the light scattering at a non-absorbing wavelength (370 nm) and a decrease in the signal at an absorbing wavelength (270 nm) indicates the formation of crystal nuclei and their growth to a detectable size (Figure S2 a) with a resultant depletion in the solution concentration. The induction times corresponds to the time when these decreases and increases in signal occur. However, when induction time measurements are conducted above GLPS, the initial presence of the drug-rich phase will cause scattering, which makes it difficult to distinguish the subsequent occurrence of crystallization. Hence, only the intensity changes at the absorbing wavelength were used to determine induction times above GLPS (Figure S2 b). As is evident from Figure S2 b, there are two drops in the apparent concentration, which have been seen for other systems containing colloidal drug-rich aggregates.⁵ The first drop in the apparent concentration is assigned to a change in the optical properties of the aggregates due to agglomeration/growth and the second drop is attributed to crystallization with a subsequent decrease of molecularly dissolved drug.

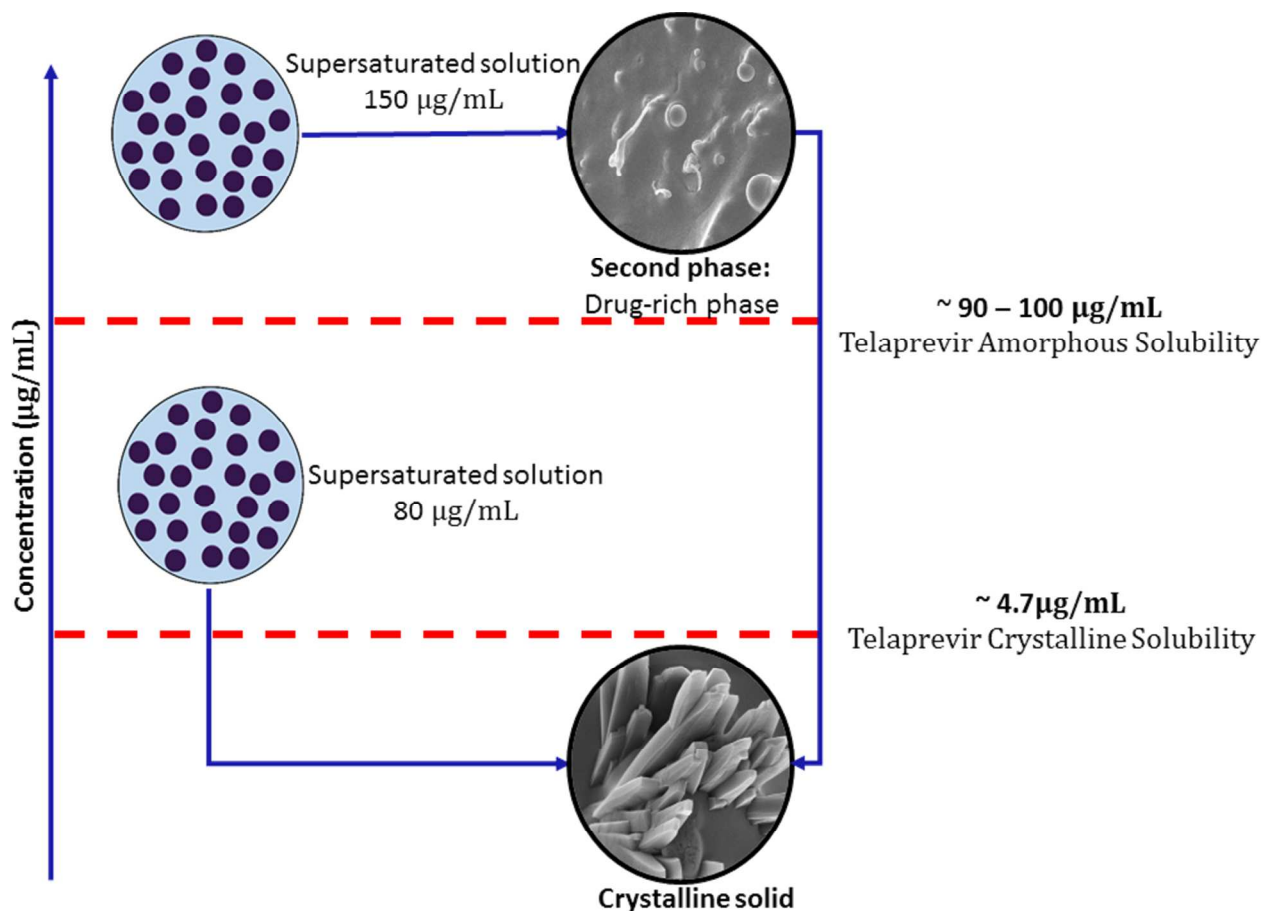


Figure S1. Schematic of supersaturated solutions of telaprevir below and above GLPS. At concentrations higher than 90 $\mu\text{g/mL}$ a glassy drug-rich phase that will then crystallized is created. Cryo-SEM showed evidence of circular aggregates at the 150 $\mu\text{g/mL}$ concentration.

Diffusion cell measurements were performed to show that the first drop in the concentration does not result in a decrease in mass flow and hence is not due to crystallization, which would reduce the supersaturation and hence the mass flow (Fig S3). When using HPMC at 5 and 50 $\mu\text{g/mL}$, the same mass flow (concentration vs time) is observed (Figure S3 b), even though two drops in the concentration are detected in the case of HPMC at 5 $\mu\text{g/mL}$ (Figure S3 a). Therefore, the first drop in the concentration, caused by the aggregation/growth of the colloidal amorphous phase is not negatively impacting the mass flow for telaprevir.

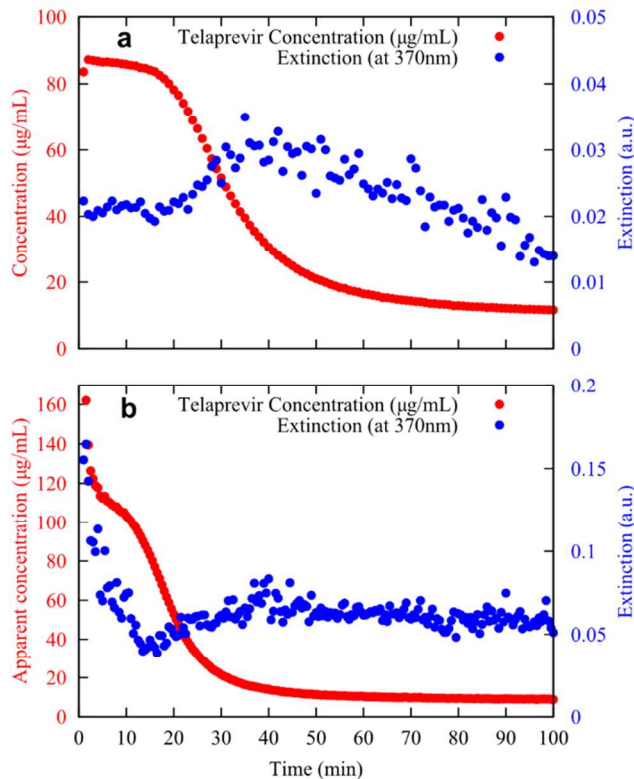


Figure S2. Representative plots of decrease in apparent concentration (red) and increase in scattering at a non-absorbing wavelength (blue) for induction time experiments in the absence of polymer. (a) at 80 µg/mL TPV which corresponds to a concentration below GLPS (b) at 150 µg/mL TPV which corresponds to a concentration above GLPS.

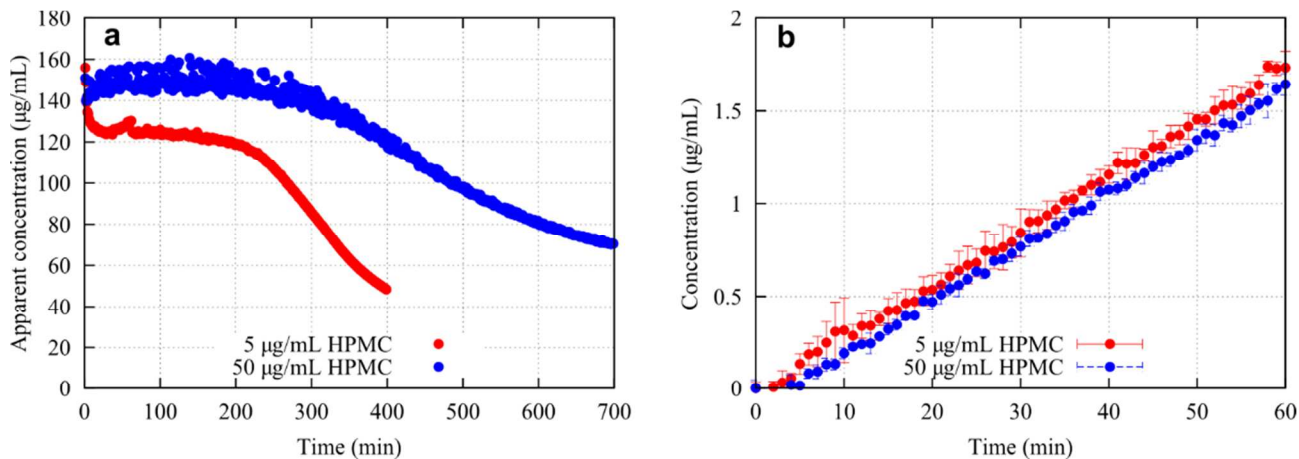


Figure S3. (a) Induction time for telaprevir in the presence of 5 and 50 µg/mL predissolved HPMC and 150 µg/mL TPV, (b) concentration as a function of time in the receiver compartment of a side by side diffusion cell (n=3).

3) Methodology Polymer Characterization

Differential Scanning Calorimetry (DSC)

To obtain the T_g values of the cellulosic polymers, DSC was performed on a TA Instruments Q100 apparatus and TA Discovery DSC using heat/cool/heat mode. Dry powders (ca. 5 mg) were loaded in Tzero™ aluminum pans. The scanning conditions were set as follows: each sample was equilibrated at 35 °C, and then heated to 150 °C at 20 °C/min. The sample was then cooled at 100 °C/min to -50 °C. During the second heating cycle, the sample was heated to 200 °C at 20 °C/min. If the heat/cool/heat mode failed to give a clear transition, modulated DSC was performed as follows: each sample was equilibrated at -50 °C, the underlying ramp heating rate was 7 °C, the oscillation amplitude was ± 1 °C, and oscillation period was 40 s.

Size exclusion chromatography (SEC)

Size exclusion chromatography, if not otherwise specified, was performed on Agilent 1260 Infinity Multi-Detector SEC using DMAc with 0.05 M LiCl as the mobile phase (50 °C) with 3 PLgel 10 μ m mixed-B 300 \times 7.5 mm columns in series. A system of multiple detectors connected in series was used for the analysis. A multi-angle laser light scattering (MALS) detector (DAWN-HELEOS II, Wyatt Technology Corporation, Goleta, CA), operating at a wavelength of 658 nm, a viscometer detector (Viscostar, Wyatt Technology Corporation, Goleta, CA), and a refractive index detector operating at a wavelength of 658 nm (Optilab T-rEX, Wyatt Technology Corporation, Goleta, CA) provided online results. Data acquisition and analysis was conducted using Astra 6 software (Wyatt Technology Corporation, Goleta, CA). Monodisperse polystyrene standard ($M_w \sim 21k$, $D \sim 1.02$) was run first in every sample series for the purpose of calibration and confirmation.

Diffusion Cell Experiments

Diffusion cell experiments were performed in a side-by-side diffusion cell. 100 mM sodium phosphate buffer with predissolved polymer (5 and 50 μ g/mL of HPMC) was used as the aqueous medium and 150 μ g/mL TPV was added in the donor compartment of the diffusion cell. The mass flow as a function of time was measured in the receiver compartment using the SI photonics UV with a 10 mm fiber optic probe. The methodology used was previously reported.³

Regenerated cellulose membranes with a molecular weight cutoff (MWCO) of 6-8 KDa were acquired from Spectrum Laboratories, Inc. (Rancho Dominguez, California).

4) Monomers Conformations

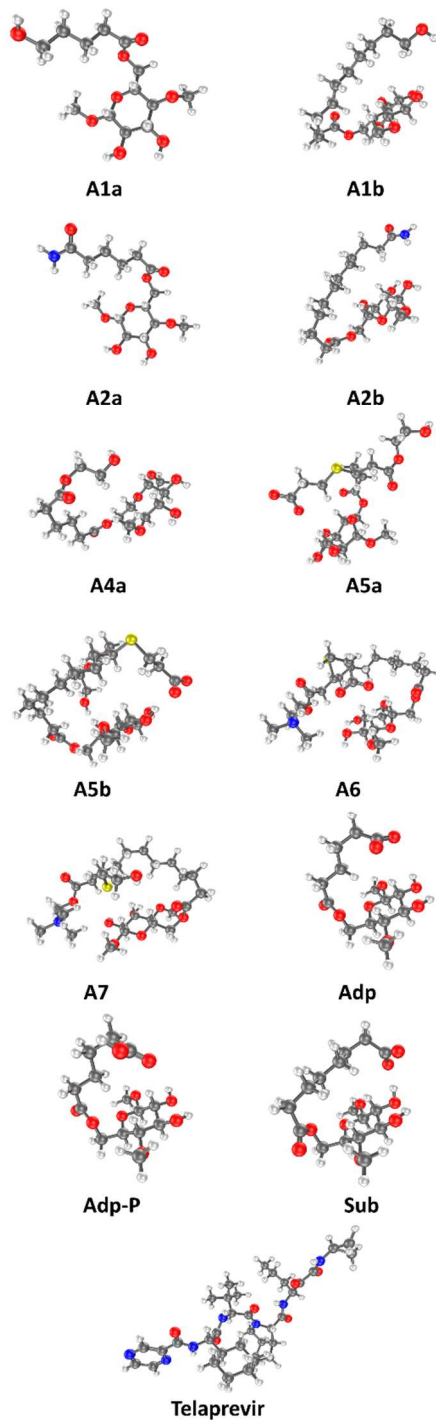


Figure S4. Monomers conformations, after conformational search and geometry optimization. Density Functional Theory (DFT) calculations were performed. The hybrid Perdew-Burke-

Ernzerhof exchange-correlation density functional (PBE0) with Pople's 6-31+G* basis set were employed in all cases. All the calculations were performed using the Polarizable Continuum Model (PCM) with the dielectric constant of water (78.39).

References

1. Meng, X.; Roy Choudhury, S.; Edgar, K. J. Multifunctional cellulose esters by olefin cross-metathesis and thiol-Michael addition. *Polym. Chem.* **2016**, *7*, (23), 3848-3856.
2. Kwong, A. D.; Kauffman, R. S.; Hurter, P.; Mueller, P. Discovery and development of telaprevir: an NS3-4A protease inhibitor for treating genotype 1 chronic hepatitis C virus. *Nature Biotechnology* **2011**, *29*, (11), 993-1003.
3. Mosquera-Giraldo, L. I.; Taylor, L. S. Glass-Liquid Phase Separation in Highly Supersaturated Aqueous Solutions of Telaprevir. *Molecular Pharmaceutics* **2015**, *12*, (2), 496-503.
4. Almeida e Sousa, L.; Reutzel-Edens, S. M.; Stephenson, G. A.; Taylor, L. S. Assessment of the Amorphous "Solubility" of a Group of Diverse Drugs Using New Experimental and Theoretical Approaches. *Molecular Pharmaceutics* **2015**, *12*, (2), 484-495.
5. Jackson, M. J.; Toth, S. J.; Kestur, U. S.; Huang, J.; Qian, F.; Hussain, M. A.; Simpson, G. J.; Taylor, L. S. Impact of Polymers on the Precipitation Behavior of Highly Supersaturated Aqueous Danazol Solutions. *Molecular Pharmaceutics* **2014**, *11*, (9), 3027-3038.